Alginate Trisaccharide Binding Sites on the Surfaceof β-Lactoglobulin Identified by NMR Spectroscopy: Implications for Molecular Network Formation

Stender, Emil G. P.; Birch, Johnny; Kjeldsen, Christian; Nielsen, Lau D.; Duus, Jens Ø.; Kragelund, Birthe B.; Svensson, Birte

Published in:
ACS Omega

Link to article, DOI:
10.1021/acsomega.8b03532

Publication date:
2019

Document Version
Publisher's PDF, also known as Version of record

ACS OMEGA

Article

Cite This: ACS Omega 2019, 4, 6165−6174

http://pubs.acs.org/journal/acsodf

Alginate Trisaccharide Binding Sites on the Surface of β-Lactoglobulin Identified by NMR Spectroscopy: Implications for Molecular Network Formation

Emil G. P. Stender,[†,∥] Johnny Birch,[†,∥] Christian Kjeldsen,[‡] Lau D. Nielsen,[§] Jens Ø. Duus,[‡] Birthe B. Kragelund,[*,§] and Birte Svensson[*,†]

[†]Enzyme and Protein Chemistry, Department of Biotechnology and Biomedicine, Technical University of Denmark, Søltofts Plads, Building 224, DK-2800 Kgs. Lyngby, Denmark

[‡]Department of Chemistry, Technical University of Denmark, Kemitorvet, Building 207, DK-2800 Kgs. Lyngby, Denmark

[§]Structural Biology and NMR Laboratory, Linderstrøm-Lang Centre for Protein Science, Department of Biology, University of Copenhagen, Ole Maaløes Vej 5, DK-2200 Copenhagen N, Denmark

Supporting Information

ABSTRACT: β-lactoglobulin (BLG) is a promiscuous protein in terms of ligand interactions, having several binding sites reported for hydrophobic biomolecules such as fatty acids, lipids, and vitamins as well as detergents. BLG also interacts with neutral and anionic oligo- and polysaccharides for which the binding sites remain to be identified. The multivalency offered by these carbohydrate ligands is expected to facilitate coacervation, an electrostatically driven liquid−liquid phase separation. Using heteronuclear single quantum coherence NMR spectroscopy and monitoring chemical shift perturbations, we observed specific binding sites of modest affinity for alginate oligosaccharides (AOSs) prepared by alginate lyase degradation. Two different AOS binding sites (site 1 and site 2) centered around K75 and K101 were identified for monomeric BLG isoform A (BLGA) at pH 2.65. In contrast, only site 1 around K75 was observed for dimeric BLGA at pH 4.0. The data suggest a pH-dependent mechanism whereby both the BLGA dimer−monomer equilibrium and electrostatic interactions are exploited. This variability allows for control of coacervation and particle formation of BLGA/alginate mixtures via directed polysaccharide bridging of AOS binding sites and has implication for molecular network formation. The results are valuable for design of polyelectrolyte-based BLG particles and coacervates for carrying nutraceuticals and modulating viscosity in dairy products by use of alginates.

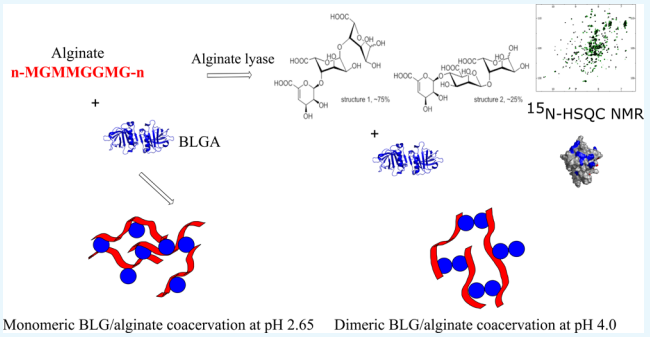

INTRODUCTION

β-Lactoglobulin (BLG) is an extensively studied lipocalin found in bovine milk,[1,2] which is able to bind a large variety of hydrophobic ligands.[3−6] The common fold of lipocalins is an 8-stranded antiparallel β-barrel that encloses an internal hydrophobic cavity, the calyx. The BLG fold includes nine β-strands, of which, strands A−H form the central calyx and strand I is involved in BLG dimer interface formation along with an α-helix (Figure 1).[7] The tertiary structure of BLG is further stabilized by two disulfide bonds (C66−C160 and C106−C119), which are buried together with a free cysteine (C121) in the hydrophobic core.[8] BLG exhibits a variable structural landscape, comprising a homodimer at neutral pH[8,9] and a monomer−dimer equilibrium at pH < 5 and is essentially monomeric at pH < 3.[10] Different hydrophobic ligands, e.g., fatty acids and retinoids,[5,6] can be accommodated inside the calyx,[3] to which access is controlled by the EF-loop that adopts a closed conformation at pH < 7.5 (Figure 1) and an open conformation at a higher pH.[10] Notably, BLG also has binding sites on the outer surface. Capryllic acid thus interacts with the loop connecting β-strands C and D (CD-loop, residues W61−C66) at the entrance to the calyx at pH 7.5,[6] while at pH 2, vitamin D_3 binds at a surface-exposed hydrophobic site (D137−R148) belonging to β-strand I, the α-helix involved at the dimerization interface, and the loop connecting the two (Figure 1).[5]

Polysaccharides are widely used as food additives such as viscosity agents, pH modulators, water retainers, and antimicrobials[11] and constitute important ligands for BLG. Below the pI (4.7−5.2),[12−17] BLG interacts with a wide range of polysaccharides, resulting in either insoluble particles[12,16,18] or liquid coacervates,[15,17] depending on the nature of the polysaccharide and the buffer composition. While particle size, strength of interaction, and formation of insoluble particles or

Received: December 17, 2018
Accepted: March 21, 2019
Published: April 2, 2019

DOI: 10.1021/acsomega.8b03532
ACS Omega 2019, 4, 6165−6174

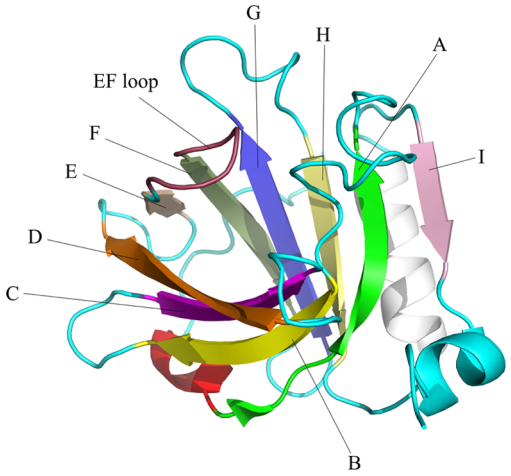

Figure 1. NMR structure of BLGA at pH 2.65 (PDB: 1DV9). β-strands A (green), B (yellow), C (purple), D (orange), E (gray), F (green-gray), G (blue), H (light yellow), and I (pink); dimerization α-helix (white); and the EF-loop (magenta) in the closed conformation.[7]

coacervates have been attributed to chemical and physicochemical characteristics of the polysaccharide,[13,18−21] the residues of BLG involved in the complex formation have so far not been identified. Positively charged patches on the BLG surface have been proposed to mediate interactions with anionic polysaccharides[13,15,16] through charge neutralization, leading to coacervation or formation of insoluble particles.[11] However, the large sizes of BLG/polysaccharide complexes have prevented detailed descriptions of their molecular structures. This knowledge void motivated the present analysis of a currently developed model system involving alginate trisaccharides binding to BLG isoform A (BLGA).[18] The major aim was to decipher the details of the molecular interactions.

Alginate is a linear, acidic polysaccharide composed of α-L-guluronic acid (G) and β-D-mannuronic acid (M)[22] organized as a copolymer with a pattern of 1,4-linked G-, M-, and M/G-blocks.[23−25] Alginate is widely used as a food additive in dairy products as a modulator of viscosity and consistency.[11] It can also protect whey proteins from gastric digestion,[26] and BLG/alginate particles have been proposed as nutraceutical carriers.[27] We previously described the pH-dependent formation of BLGA/alginate particles and in that connection also showed that the model alginate trisaccharides (AOSs), prepared by alginate lyase degradation, bound to BLGA at pH values 3.0 and 4.0 with K_d values of 1.1 and 0.6 mM, respectively.[18] To explain the interaction in more detail to ultimately enable unraveling of the coacervation mechanisms, the structures of the AOSs are identified here and their binding sites on BLGA decomposed using NMR spectroscopy under BLGA monomer- and dimer-forming conditions at pH values 2.65 and 4.0. Besides mapping of the AOS binding sites to the BLGA surface, distinct pH-dependent binding site differences related to the monomer−dimer equilibrium were seen, which may be relevant for modulating the coacervation behavior of BLGA.

RESULTS

Structure Determination of AOSs, an Alginate Model. Alginate oligosaccharides were prepared by degradation using endoacting alginate lyase, and the di- and trisaccharide end

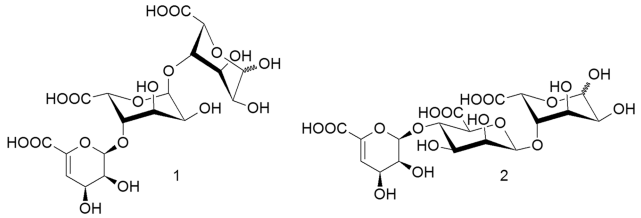

Figure 2. Structures of alginate trisaccharides (AOSs). **1** is the major component (~75%) (4-deoxy-α-L-erythro-hex-4-enopyranosyluronate)-(1,4)-(α-L-gulopyranosyluronate)-(1,4)-(L-gulopyranosyluronate); **2** is the minor component (~25%) (4-deoxy-α-L-erythro-hex-4-enopyranosyluronate)-(1,4)-(β-D-mannopyranosyluronate)-(1,4)-(L-gulopyranosyluronate).

products were separated by high-performance liquid chromatography (HPLC)[18] (see Materials and Methods), resulting in 12 mg of trisaccharides (AOSs) from 100 mg of alginate (Figure S1). Structural analysis by NMR revealed a mixture of two AOSs with G at the reducing end. The dominant species (**1**) (75%) had G as the central residue, whereas the minor species (**2**) (25%) had M (Figure 2). As the lyase removes the 4-OH group and the C-5 proton by β-elimination,[28] the C5 epimers β-D-mannuronic acid and α-L-guluronic acid lead to the same nonreducing end product, 4-deoxy-α-L-erythro-hex-4-enopyranosyluronic acid (Figure 2; Table S1; Figures S2−S7). The structure of these compounds has previously been solved by NMR, and the assigned chemical shifts are in good correlation with previous results.[29,30]

BLGA Has Two Different Binding Sites for AOSs at Low pH. AOS binding to BLGA was investigated under different conditions[18] than those used for earlier NMR chemical shift assignments of BLGA.[7] Therefore, BLGA was prepared with the same primary structure as earlier and the first NMR spectra were recorded under the same conditions as those used in that study. Subsequently, the chemical shifts were followed under conditions used to measure binding via chemical shift perturbations upon addition of AOSs. BLGA has 165 residues including eight prolines and the additional three residues of the N-terminal (see Materials and Methods, Figure S1). Accordingly, excluding the fast exchanging N-terminal and the side chain resonances, a total of 156 resonance peaks are expected. Indeed, the $^{1}H,^{15}N$-heteronuclear single quantum coherence (HSQC) spectrum recorded at pH 2.65 showed 156 dispersed peaks, of which 145 were unambiguously assigned to BLGA residues (BMRB 27668, Figure S8). Due to overlap/ambiguities (Y2, K8, N63, C160) and lack of assignment in the reported shift list (L22, E157, E158, I162),[7] nine residues of BLGA were left unassigned. Importantly, the assigned chemical shifts were in good agreement with those previously reported for BLGA[7] (Figure S9, Tables S2, S3), indicative of correctly folded recombinant BLGA WT.

To map where the oligosaccharides bind on the monomer, BLGA was titrated with AOSs at pH 2.65, reaching a molar concentration of 15.5 mM (Figure 3A). Although distinct chemical shift perturbations were seen, the amplitudes of the shifts were generally small. Due to weak binding, saturation was not achieved and fitting to a classical binding model was not possible (Figure S10). Still, chemical shift perturbation analysis by addition of AOSs (Figure 4) identified affected residues particularly in three surface-exposed regions, D11−K14 (N-terminal region), K101−Y102 (FG-loop), and E127−D137 (dimerization α-helix) (Figure 1). Single affected

DOI: 10.1021/acsomega.8b03532
ACS Omega 2019, 4, 6165−6174

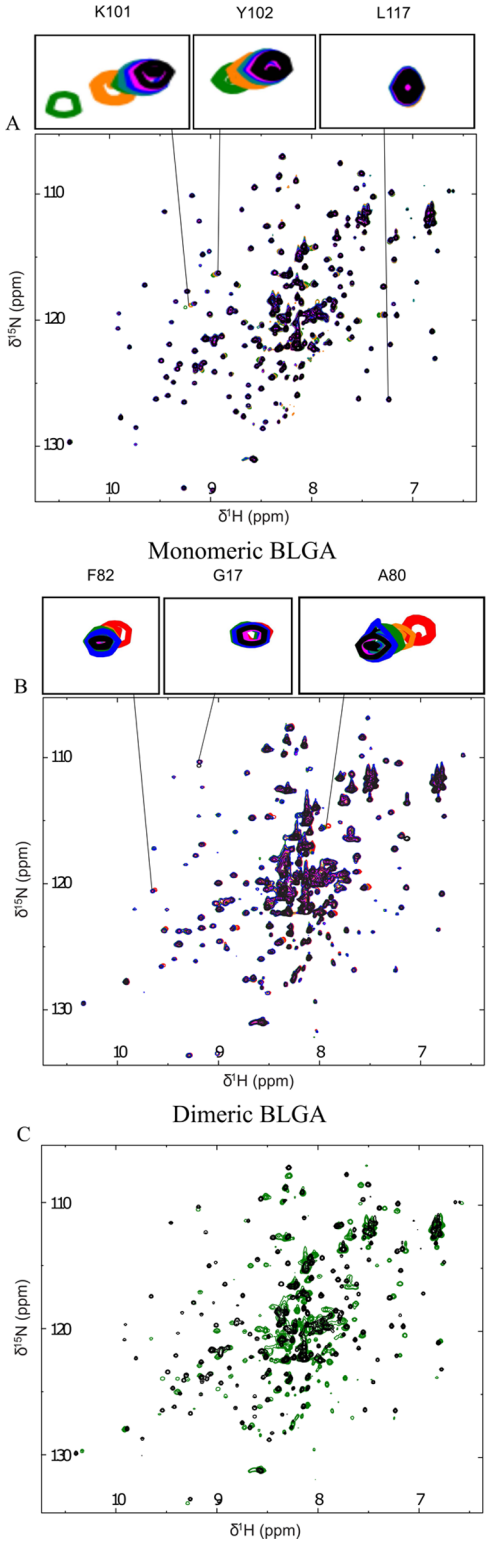

Figure 3. $^{1}H,^{15}N$-HSQC spectra of BLGA WT titrated with AOSs at pH values 2.65 and 4.0. (A) 0 mM AOSs (black) and 15.5 mM AOSs (green) at pH 2.65. (B) 0 mM AOSs (black) and 15.5 mM AOSs (red) at pH 4.0. (C) Overlay of $^{1}H,^{15}N$-HSQC spectra of BLGA WT at pH 2.65 (black) and pH 4.0 (green).

residues outside these regions were also observed, including S30 (AB-loop), K75 (β-strand D), I84 (FG-loop), and L149 (β-strand I), as well as perturbation of three unassigned peaks (Figure 4, Table 1). Although most of the regions and residues directly contain or have neighboring positively charged residues, mainly lysine, there were several lysines on the BLGA surface that remained unperturbed, e.g., K39, K47, K48, K60, K69, and K70.

Based on these observations, two binding sites, site 1 and site 2, were defined, which, together with the anionic character of AOSs, motivated the production of BLGA single variants, K8A, K75A, and K101A, to investigate the effect on binding by removing a specific positive charge. K8A was chosen based on its location spatially close to K14 and K75 and because it was unassigned in our work due to overlap. K8 was thus hypothesized to be one of the three unassigned spin systems undergoing chemical shift perturbations by addition of AOSs. In the $^{1}H,^{15}N$-HSQC spectrum of BLGA K8A, some peak overlap was observed, but it still allowed for K8 assignment (Figure 5A). Notably, after successful assignment, it was clear that K8 was unperturbed at pH 2.65 by addition of AOSs (Figure 4).

The conformational integrity of unlabeled recombinant BLGA WT and mutant proteins was assessed by far-UV circular dichroism (CD). As expected for the β-sheet-rich BLGA,[31] a global minimum at 216−218 nm was observed and only very small differences from WT were seen for K8A and K75A (Figure S11). By contrast, the fold of the K101A variant was clearly compromised as deduced from the shifted CD minimum (Figure S11) in agreement with extensive peak collapse in the $^{1}H,^{15}N$-HSQC spectrum, indicative of a partially unfolded structure (Figure 5C). AOS binding analysis was therefore not pursued for BLGA K101A. At pH 2.65, AOSs elicited a similar chemical shift perturbation for K8A, K75A, and WT BLGA (Table 1). Thus, not one single residue appeared to be solely responsible for the binding of AOSs to BLGA.

Two AOS binding sites were identified on the surface of monomeric BLGA at pH 2.65, site 1 and site 2 (Figure 4, see also Figure 7). Except for S30 (AB-loop) and L149 (β-strand I) (Table 1, Figure 4), most of the involved residues of BLGA are situated outside the dimerization interface, i.e., the AB-loop (S27−V41) and β-strand I (I147−F150).[32] Subsequently, the influence of pH on AOS binding was investigated at pH 4.0 where BLGA is mostly in the dimeric form.[10]

pH Tunes Alginate Binding to BLGA and Controls Coacervation. The effect of BLGA dimerization on the binding of AOSs in a dairy-relevant pH range was investigated by chemical shift perturbation at pH 4.0.[33] First, BLGA resonances were assigned at pH 4.0 by titration from pH 2.65 to 3.2 and 4.0 (Figure 3C; Figure S12, Tables S2, S4). Here, at pH 4.0, we obtained unambiguous assignments of 132 residues, compared to 145 residues at pH 2.65. As expected, this increase in pH caused BLGA to dimerize, which seriously affected line widths for several peaks, resulting in assignments of only 132 residues (Table S4, BMRB no: 27668). Mapping these missing assignments onto the BLGA structure clearly showed that residues with broadened peaks located distinctly to the known dimerization interface (Figure 7C). Next, AOSs were added by titration and chemical shift perturbations were analyzed (Figures 6 and 3B). Compared to the BLGA monomer, distinct differences were observed. Notably, Y102 in site 2 was no longer affected by AOS binding, and K101 was less affected at pH 4.0 than at pH 2.65 (Figure 6). By contrast, K75 in site 1 retained a significant chemical shift perturbation at pH 4.0. Moreover, residues belonging to the α-helix contributing to the dimerization interface were unperturbed by

DOI: 10.1021/acsomega.8b03532
ACS Omega 2019, 4, 6165−6174

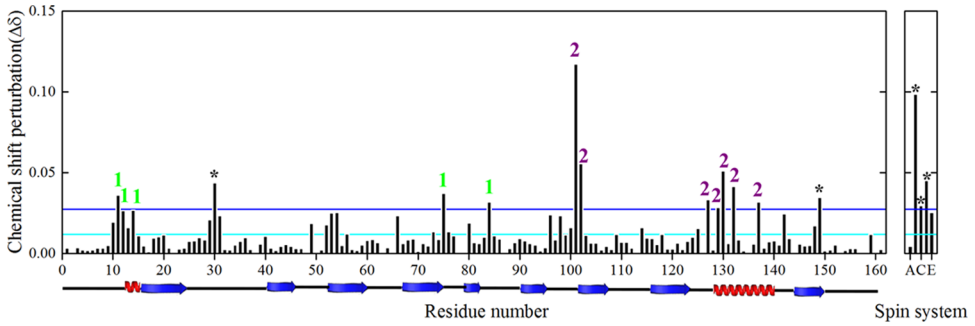

Figure 4. Chemical shift perturbation analysis of BLGA WT upon addition of AOSs at pH 2.65. The cyan line represents the average chemical shift, and the blue line represents the average chemical shift perturbation plus 1 standard deviation. A schematic representation of the secondary structure of BLGA is shown below the *x*-axis. Digit 1 (green) represents residues involved in site 1 around K75, digit 2 (purple) represents residues involved in site 2 around K101, and the stars indicate single residues undergoing significant chemical shift perturbations.

AOS binding, whereas the signal for D129 was lost (Tables 1 and S4). A few peaks, including those of the surface-exposed K8 and K83 (Table 1), which were unaffected at pH 2.65, were changed by AOS binding at pH 4.0. Notably, also the buried A80 was affected by binding, which may be due to changes in K8, which is located in the flexible, disordered N-terminal region,[7,8] shielding A80. At pH 4.0, K8 was clearly involved in AOS binding. Taken together, these comparative data highlight that AOS exploits the surface of BLGA in a pH-dependent manner and that the monomer and the dimer of BLGA bind differently to AOSs.

Mapping AOS-induced chemical shift perturbations at pH values 2.65 and 4.0 to the surface of BLGA identified two areas at pH 2.65 (Figure 7), site 1 constituted by D11, E12, K14, and K75 (BLGA N-terminal region and DE-loop) and site 2 constituted by K101, Y102, E126, D128, and D129 (FG-loop and H-dimerization α-helix loop). Notably, at pH 4.0, residues of site 2 surrounding K101 appeared unaffected by addition of AOSs and the shift for K101 was of much smaller amplitude than at pH 2.65. A change in pH to 4.0 is assumed to affect the protonation state of the acidic side chains. Using PROpKa,[34] the pH change is suggested to partially deprotonate E126, D128, and D129. The pK_a values calculated for these residues in the monomeric (PDB 1DV9) BLGA were D128, 2.52; D129, 4.79; and E126, 4.80 and for dimeric (PDB: 1BEB) BLGA, D128, 3.69; D129, 4.11; and E126, 4.18. Considering the prediction accuracy of PROpKa, we note that these values are similar to those of the free amino acids (Glu, pK_a 4.07 and Asp, pK_a 3.90). Overall, it is reasonable to assume partial deprotonation at pH 4.0. This alters the electrostatic surface of site 2, rendering it binding-incompetent due to charge−charge repulsion between BLGA and the anionic AOSs. Moreover, E126, D128, and D129 are located close to the dimerization interface. At pH 4.0, site 1 surrounding K75 also changes, as K14 no longer contributes, while K8, A80, K83, F82, and D53 appear affected.

Turbidity measurements on BLGA and alginate have been shown to gauge coacervate formation.[18,20] Since the change in AOS-induced chemical shift perturbations for both K8A and K75A was indistinguishable from WT (Table 1), turbidimetry was performed on BLGA WT, K8A, and K75A at varying alginate concentrations to confirm that the mutations have little effect on the ALG/BLGA interaction. K8A and K75A BLGA gave marginally less protein remaining in solution than WT, albeit BLGA WT at the higher alginate concentrations displayed increased turbidity compared to the two variants (Figure 8). The reason for this may be lower affinity of BLGA variants for alginate, resulting in smaller and/or fewer particles than with WT. The mutant proteins may also have lower solubility due to lower surface charge.

DISCUSSION

BLG is known to exploit different binding sites for a wide range of molecules spanning from hydrophobic ligands accommodated inside the calyx[3] to vitamins binding on the surface.[5] The presently identified AOS binding sites are distinct from previously reported binding areas on the surface of BLGA and the first accommodating carbohydrates.[5,6] Notably, a subset of the lysines is consistently involved in AOS binding (K14, K75, K83, K101 at pH 2.65 and K8, K75, K101 at pH 4.0). However, many of the 15 surface-exposed lysines[7] appear unaffected by the presence of AOSs. This highlights that the probed interactions are specific and not a mere electrostatic effect, which is also supported by the mutational removal of a single cationic side chain having little effect on binding, suggesting that other types and not just electrostatic forces are involved in the interaction. Some of the unaffected lysines may engage in local surface electrostatics of their immediate environment, in this way preventing interaction with AOSs. BLG has previously been shown to undergo a conformational change to a more α-helical structure induced by anionic lipids at pH values 4.6 and 2.6.[35] However, addition of AOSs did not elicit large changes in the NMR spectra, indicative of helix formation (Figure 3). K_d values of AOS binding to BLGA were determined previously by isothermal titration calorimetry (ITC) to 1.1 and 0.6 mM at pH 3.0 and 4.0, respectively.[18] However, none of the present chemical shift perturbations reached saturation to allow for determination of K_d (Figure S10). Presumably, this is due to the 5-fold higher ionic strength used in the NMR compared to the ITC experiments, weakening the electrostatic interactions between AOSs and BLGA.[16,18,36]

Binding of aroma compounds onto the surface of BLG at pH 2.0 was described by NMR,[37] identifying two hydrophobic binding sites, one for γ-decalactone involving K47, L57, K70, and I72 and one for β-ionone involving K60, Y102, L104, and E129.[37] Both sites are located in the hydrophobic region between β-strand G, the dimerization α-helix, and β-strand I. The positions of these binding sites are distinctly different from those determined for the AOSs, although Y102 is shared. Notably, BLGA is reported to catalyze lipofuscin formation using K60 and K69 as well as K77 and K91 as catalytic

DOI: 10.1021/acsomega.8b03532
ACS Omega 2019, 4, 6165−6174

Table 1. Chemical Shift Perturbations Above the Average Chemical Shift Plus One Standard Deviation in the ^{1}H,^{15}N-HSQC Spectrum of BLGA in the Presence of 15.5 mM AOSs[a]

	pH	K8	G9	L10	D11	I12	K14	S30	V41	D53	L57	K75	A80	F82	K83	D85	K101	Y102	E114	L117	E127	D129	D130	A132	D137	L149	{B}	{C}	{D}
BLGA WT	2.65				x	x	x	x				x					x	x			x	x	x	x	x	x	x	x
BLGA WT	4.0	x	x	x				[x]	x	x	x	x	x	x	x	x	x		x	x		[x]		x		x		x	
BLG K8A	2.65				x	x	x	x				x					x	x			x	x	x	x	x	x	x	x	x
BLG K75A	2.65				x	x	x	x				x					x	x			x	x	x	x	x	x	x	x	x

[a][x] indicates peaks lost at pH 4.0.

residues.[38] Also, none of these residues were found to interact with the AOSs, even though side chain assignments are needed to fully confirm this conclusion.

Charged patches on BLG were previously suggested to engage in interaction with anionic polysaccharides,[13,15,16,18,20] and binding regions for anionic polysaccharides were hypothesized to include residues A1−K14, V41−K60, T76−K83, and A132−R148.[15,16] Notably, at pH 4.0, the AOS-perturbed residues in BLGA are K8, G9, D11, D53, K75, A80, F82, K83, and D85, whereas no residues from the stretch V41−K60 underwent noteworthy chemical shift perturbation, except the surface-exposed D53 and the buried V41 and L57 (Figure 6). At pH 2.65, two AOS binding areas are identified on BLGA, of which site 1 remains as the sole, albeit rearranged, binding site at pH 4.0. However, the AOSs do bind near residues from the segments A1−K14 and K75−D85 at both pH 4.0 and 2.65, suggesting these regions to be the main sites. In addition, at pH 2.65, significant chemical shift perturbation occurred in the region A132−R148 as well as around K101−Y102 in site 2, but these disappeared at pH 4.0 (Figure 6). The observation of two binding sites at pH 2.65 is in agreement with previous ITC stoichiometry of two BLGA AOS binding sites at pH 3.0 and one at pH 4.0.[18]

The charged state of AOS is very important for a valid extrapolation of the AOS binding sites to alginate/BLGA interaction and subsequent coacervation. The pK_a values of M and G monosaccharides are 3.38 and 3.65, respectively.[39] Thus, there is a possibility that AOS could be neutral at pH 2.65. The individual pK_a values of the acid groups in the sugar units and the charged state of the molecule were predicted using Chemicalize. At pH 2.65, it is predicted that 64.21% of the population is charged (25.2% −2, 39.01% −1), and at pH 4, 100% of the molecules are charged (77.55% −3, 21.11% −2, 1.34% −1). Thus, the AOS should be charged under all conditions used in this study and the results thus enable extrapolation to alginate binding. site 1 is also affected at both pH 2.65 and 4, indicative of ionic contribution in the interaction at both pHs. The presence of the double bond at the nonreducing end of the trisaccharides is a consequence of the enzymatic degradation as no alginate hydrolase has been discovered to date.[40] It will cause a change in the sugar ring that goes from being in a chair conformation to a boat conformation. This combined with short trisaccharides will have significant border effects that are not found with the polysaccharide. The AOS, however, is the only alginate oligosaccharide published to date that does not form insoluble particles with BLGA, while the interaction with BLGA remains.[18] This is why AOS was chosen as a model system for NMR studies. Enzymatic degradation affords a greater control over the polymerization as opposed to partial acid hydrolysis and was chosen for this reason.

AOSs are a mixture of two anionic trisaccharides (Figure 2), which are expected to interact with positively charged residues such as lysines as found for other anionic oligosaccharide protein complexes.[41] In BLGA also, hydrophobic residues undergo chemical shift perturbations including Y102 at pH 2.65 and L10, A80, and F82 at pH 4.0. This is also supported by the little difference observed by mutating K8 and K75 in the interaction sites (Table 1 and Figure 8). This suggests that other types of interactions are involved in AOS binding to BLGA, thus going beyond what is classically seen for oppositely charged flexible polymers.[42] This could be a consequence of BLGA having a well-defined tertiary structure

DOI: 10.1021/acsomega.8b03532
ACS Omega 2019, 4, 6165−6174

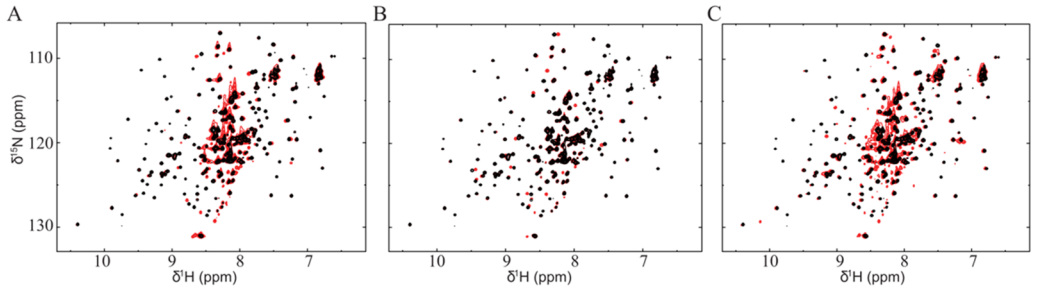

Figure 5. $^{1}H,^{15}N$-HSQC spectrum of BLGA WT (black) overlaid with $^{1}H,^{15}N$-HSQC spectra of BLGA mutants (in red): (A) K8A, (B) K75A, and (C) K101A at pH 2.65.

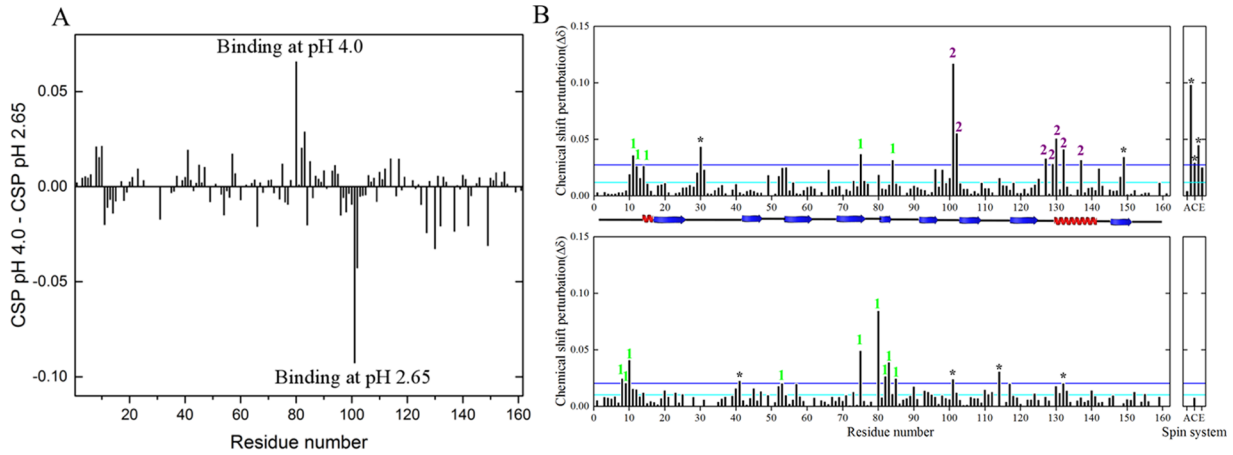

Figure 6. Differences in chemical shift perturbation of BLGA WT/AOS interaction at pH 2.65 and 4.0. (A) Chemical shift perturbation at pH 4.0 with chemical shift perturbation at pH 2.65 subtracted. (B) Chemical shift perturbation at pH 2.65 (top) and pH 4.0 (bottom). Digit 1 represents residues of site 1 located around K75, digit 2 represents residues at site 2 around K101, and stars are single residue significant chemical shifts.

at pH values 2.65 and 4.0[10,43] and therefore charged or hydrophobic residues cannot move freely relative to the binding area upon interaction with AOSs.

The mutational analysis of alginate/BLGA binding/coacervation did not reveal big differences between the mutant proteins and WT (Figure 8). However, the observed differences in the alginate concentration required to reach a saturation could indicate a change in binding stoichiometry; something that will be needed to be addressed in later studies.

Overall, these results identify binding sites on BLGA for anionic oligosaccharides and hence also polysaccharides, which are dependent on the pH and thus on the oligomeric state of BLGA. Through binding of longer polysaccharides, this forms the basis for coacervate formation. Thus, the pH dependence is one way to regulate the behavior of the coacervates, opening up for the design of polysaccharides aimed toward specific coacervate properties using BLGA. Modulating charge density and hydrophobicity of the carbohydrate ligands to target the binding sites can enable selection for specific higher-order assemblies.

CONCLUSIONS

Two surface-exposed AOS binding sites on monomeric BLGA centered around K75 (site 1) and K101 (site 2) were identified. The sites are distinctly different from previously reported binding sites on BLG for other compounds. Notably, in the dimeric BLGA, only site 1 is functional at pH 4.0. Although the AOSs/BLGA interaction is electrostatically driven, the binding sites are specific and not structurally dynamic, suggesting that other types of important interactions occur, e.g., stacking interactions between monosaccharide rings and aromatic side chains. A further scrutiny of these interactions by mutations can help elucidate their importance including their influence on macromolecular particle formation. Overall, the distinct BLGA binding sites and their pH dependence are fundamental characteristics that can help guide design of polyelectrolyte carbohydrates to achieve desirable coacervate behavior.

MATERIALS AND METHODS

Preparation of Alginate Oligosaccharides (AOSs). AOSs were prepared essentially as described.[18] Briefly, 10 mg mL^{-1} alginate ($\bar{M}_n$ = 40 kDa = M/G ratio = 0.6, and polydispersity = 2.6; kind gift of Finn Madsen, DuPont Nutrition Biosciences, Brabrand, Denmark) was incubated with endoacting alginate lyase from *Sphingomonas* sp. (Megazymes, Ireland) at 42 °C for 6.5 h, followed by enzyme inactivation (90 °C, 10 min), centrifugation (20 000*g*, 10 min), and desalting of the supernatant into water (Hiprep Desalt 26/10; GE Healthcare). Oligosaccharide products were monitored spectrophotometrically at 235 nm.[18] The fractions containing AOSs were added acetonitrile to 50% (v/v) and purified by HPLC (TSKgel Amide-80 column 5 μm particle size; 4.6 by 250 mm with 4.6 × 10 mm guard column (Tosoh, Japan); Ultimate 3000 HPLC (Dionex, CA) equipped with RI-101 refractive index detector (Showa Denko, Japan)) eluted by 70% (v/v) acetonitrile in water as mobile phase at 70 °C at a flow rate of 1 mL min^{-1}. AOSs were quantified using the phenol sulfuric acid method.[18,44] Purity was assessed by thin layer chromatography (TLC; silica gel 60 F_{254}; Merck) 2 × 3

DOI: 10.1021/acsomega.8b03532
ACS Omega 2019, 4, 6165−6174

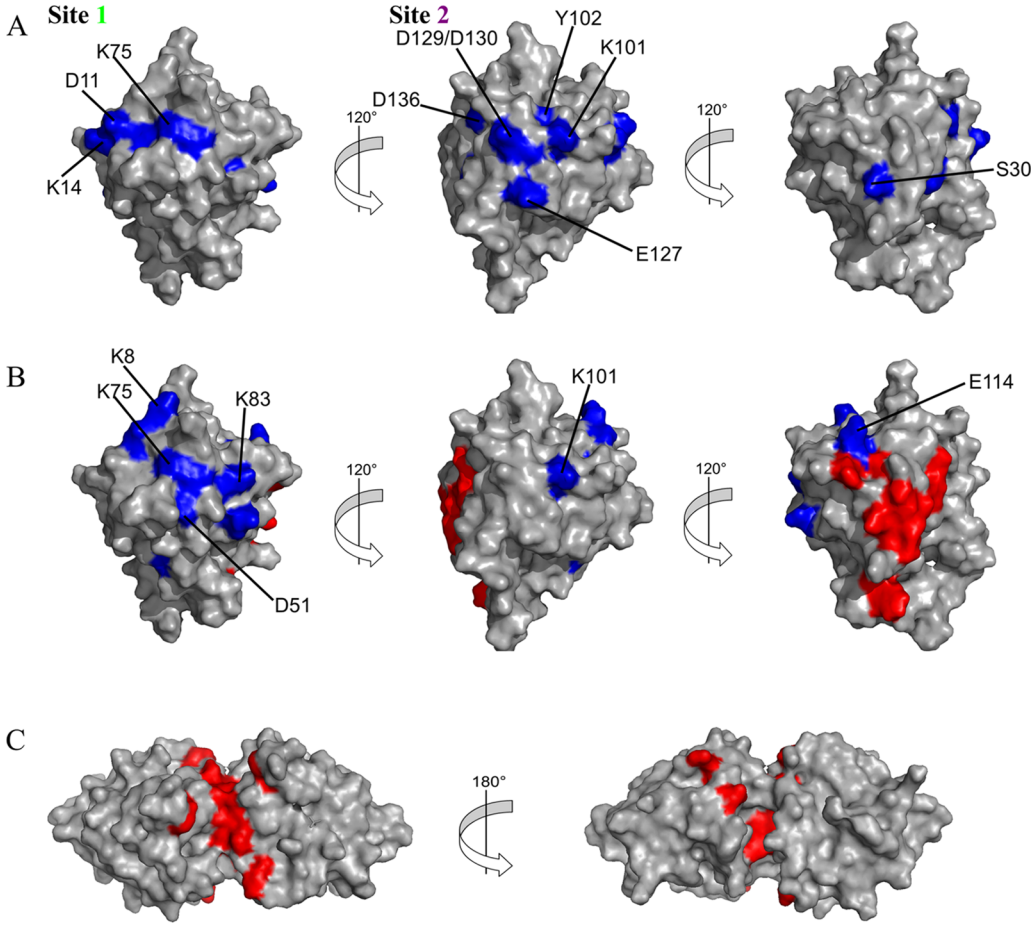

Figure 7. Mapping of AOS-induced chemical shift perturbations (blue) onto the surface of monomeric BLGA WT (PDB: 1DV9)[7] at (A) pH 2.65 and (B) pH 4.0. (C) Residues assigned to peaks lost during the pH titration (pH 2.65 to 3.2 to 4.0) are in red and also mapped to the BLGA dimer (PDB: 1BEB).[8]

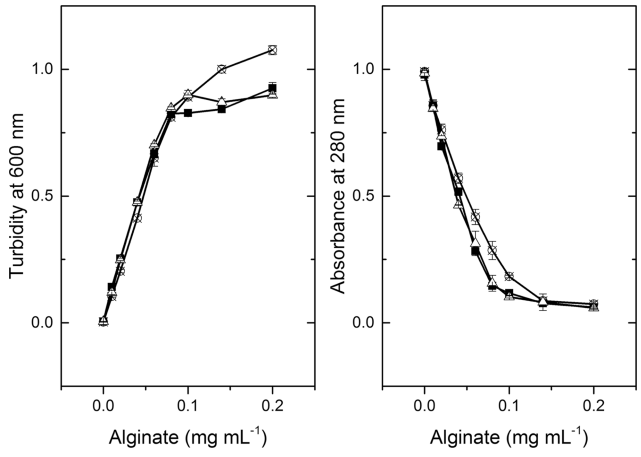

Figure 8. Turbidity (600 nm) of BLGA WT and variants mixed with alginate at pH 4.0 and absorbance (280 nm) of supernatants after centrifugation (see Materials and Methods): BLGA WT (circle), K75A (square), and K8A (triangle).

μL spotted effluent, developed twice in 50% butanol/25% acetic acid/25% MilliQ water and visualized by taring (300 °C) in 10% sulfuric acid, 80% ethanol, 8% H_2O, and 2% orcinol (Supporting Information, Figure S1).

pK_a values of the acid groups in AOSs were predicted by submitting the structure to chemicalize.com (ChemAxon, 06/02-2019).

BLGA Cloning, Mutagenesis, and *Pichia pastoris* Transformation. The vector pPICZαA harboring the gene encoding BLGA (UniProt: P02754) was optimized for *P. pastoris* to produce a recombinant BLGA variant with the N-terminal extension EAE (here numbered −1 to −3) and three point mutations, changing L_1I_2 to A_1,Y_2 and the V105F (Figure S1). These changes were done to enable transfer of assignments reported previously for structure determination of BLGA by NMR.[7] The full primary structure of this BLGA variant is given in the Supporting Information. The DNA sequence encoding the BLGA V105F (referred to as BLGA) was cloned in-frame with the *Saccharomyces cerevisiae* α-mating factor to give pPICZαA−BLGA (purchased from GeneArt; Thermofisher). An Xhoi restriction site was introduced after the α-factor gene to avoid additional amino acids to remain after cleaving off the α-factor. Single BLGA mutants K8A, K75A, and K101A were made by site-directed mutagenesis (Quick Change lightning mutagenesis kit; Agilent) using the primers (purchased from Eurofins Genomic; Germany) K8A 5′cgtcacccagaccatgcagggtttggatatcca3′; K8A_anti 5′tggatatccaaaccctgcatggtctgggtgacg3′; K75A 5′gtgctcagaagaagatcattgcagaagcaaccaagatccctg3′; K75A_anti 5′cagggatcttggttgcttctgcaatgatcttcttctgagcac3′, K101A 5′ggttttggacaccgactacaaagcgtacttgttgttctgcatg3′, and K101A_anti

DOI: 10.1021/acsomega.8b03532
ACS Omega 2019, 4, 6165−6174

5′catgcagaacaacaagtacgctttgtagtcggtgtccaaaacc3′. Wild-type (WT) and mutant plasmids were transformed into *Escherichia coli* DH5α by heat shock and selected for zeocin resistance (Novagen, U.K.), and the mutations were confirmed by sequencing (GATC Biotech, Germany). pPICZαA−BLGA WT and mutant plasmids were linearized using *Pme*I and transfected into *P. pastoris X*-33 by electroporation (EasySelect Pichia Expression Kit; Invitrogen). Transformants were selected on zeocin containing yeast extract peptone dextrose (YDP) agar plates incubated 3 days at 30 °C.

Production of Isotope-Labeled Recombinant BLGA. Eight clones from each *P. pastoris* transformation were restreaked on YDP agar zeocin plates and selected for expression level in 50 mL of buffered minimal methanol medium (BMM: 0.1 M K_2HPO_3/KH_2PO_3 (KPi) pH 6.0, 0.34% (w/v) yeast nitrogen base without amino acids and ammonium chloride, 4×10^{-5}% (w/v) biotin, 1% ammonium sulfate, 0.5% (v/v) glycerol), growing for 5 days at 22 °C evaluated on aliquots removed with 24 h intervals and analyzed by sodium dodecyl sulfate-polyacrylamide gel electrophoresis (SDS-PAGE). The transformants secreting the highest amount of protein were propagated in 25 mL of buffered glycerol-complex medium (BMGY: 1% (w/v) yeast extract, 2% (w/v) peptone, 0.1 M KPI pH 6.0, 1.34% (w/v) yeast nitrogen base, 4×10^{-5}% (w/v) biotin, 1% (v/v) glycerol) (30 °C, 150 rpm) until OD_{600} = 2−6, inoculated into 1 L BMGY medium in baffled 3 L shake flasks, and grown until OD_{600} = 2−6. Cells were harvested by centrifugation (1500*g*, 5 min, 22 °C), resuspended in 1 L of BMM medium, incubated 110 h (22 °C, 150 rpm), and methanol being added to 0.5% (v/v) every 24 h. Cells were pelleted (10 000*g*, 30 min, 4 °C), and the supernatant was filtered (0.45 μm) and concentrated by cross-flow filtration (SARTOFLOW Slice 200 Benchtop System, 5 kDa Hydrostart ultrafiltration cassette at 4 °C; Sartorius, Germany). Protein concentration was determined spectrophotometrically using a predicted molar extinction coefficient of 18 700 M^{-1} cm^{-1} (Protparam).[45] Conformational integrity of BLGA variants was confirmed by circular dichroism spectroscopy. For NMR analysis ^{15}N-labeled BLGA was produced essentially as described above in 2 L of BMM (0.1 M KPi pH 6.0, 0.34% (w/v) yeast nitrogen base without amino acids and ammonium chloride, 4×10^{-5}% (w/v) biotin, 1% ^{15}N-ammonium sulfate (Cambridge Isotope Laboratories Inc., Andover), 0.5% (v/v) glycerol).

Purification of Recombinant BLGA WT and Mutants. All steps were performed at 4 °C. Concentrated culture supernatant was buffer-exchanged to 50 mM KPi pH 6.0, 150 mM NaCl (Hiprep Desalt column 26/10; GE Healthcare) at a flow rate of 2 mL min^{-1} and concentrated (3 kDa cutoff, Amicon Ultra 15 centrifugal filter; Merck). Recombinant BLGA WT and mutant proteins were purified by size exclusion chromatography (Hiload Superdex 75 26/60; GE Healthcare) at a flow rate of 1.4 mL min^{-1} in 50 mM KPi pH 6.0 and 150 mM NaCl and dialyzed (MilliQ water, 3 kDa cutoff Spectra/Por membrane; Spectrumlabs) by 3 × 100-fold dilution, each for 4 h, evaluated by SDS-PAGE to be >95% pure (data not shown), lyophilized, and stored at −20 °C until use. For NMR experiments, proteins were dissolved in 55 mM KPi pH 2.65, 3.2, or 4.0 and dialyzed against the buffer (as above). Yields of purified BLGA WT, K8A, K75A, and K101A were 40.4, 20.6, 35.2, and 6.3 mg, respectively, per liter of culture containing ^{15}N-ammonium sulfate.

Circular Dichroism Spectroscopy. Lyophilized BLGA WT and mutant proteins were dissolved in 10 mM NaPi pH 7.0, centrifuged (20 000*g*, 20 min, 4 °C), and dialyzed (3 kDa cutoff, Spectra/Por membrane; Spectrumlabs) 3 × 100-fold dilution, each against the buffer for >4 h, at 4 °C. Far-UV CD spectra were recorded at 250−190 nm in a 1 mm quartz cuvette (50 nm min^{-1}, 1 nm bandwidth, 2 s response time, 25 °C; Jasco J810 Spectropolarimeter, Peltier controlled). Ten scans were averaged, and a buffer background recorded using identical parameters was subtracted. The molar ellipticity was calculated by

$$[\theta] = 100 \times \frac{\theta_\lambda}{m} \times d$$

where m is the molar protein concentration, θ is the ellipticity at wavelength λ, and d is the path length in centimeter.[31]

NMR of BLGA WT and Mutant Proteins. ^{15}N-BLGA WT and mutant proteins were diluted to 50 mM KPi H_2O/D_2O (9/1 v/v) and 0.1 mM 2,2-dimethyl-2-silapentanesulfonic acid (DSS) and centrifuged (12 000*g*, 20 min, 4 °C) prior to analysis by NMR spectroscopy in 5 mm Shigemi microtubes. The buffer was chosen to match the conditions used by Uhrínová et al.[7] and to ensure consistent pH values outside the main buffering range of the buffer. Upon addition of ligand, pH was corrected in all samples prior to the measurement and measured immediately after, to secure consistency. BLGA WT is monomeric[10] and stable for many days at pH 2.65,[7] while a significant amount of dimer is present at pH values 3.2 and 4.0.[10] The ^{1}H, ^{15}N-heteronuclear single quantum coherence (HSQC) spectra were recorded on an 800 MHz Varian INOVA spectrometer equipped with a 5 mm triple resonance room temperature probe with a Z-field gradient at 37 °C[46] using a Varian/Agilent BioPack sequence or on a 600 MHz Bruker AVANCE system equipped with a cryoprobe. Recorded free induction decays were processed with nmrPipe.[47] Proton chemical shifts were referenced to internal DSS at 0.00 ppm and indirectly using gyromagnetic ratios for ^{15}N and ^{13}C chemical shifts.

NMR Assignment and Chemical Shift Perturbation Analysis. Assignments of N and H^N nuclei of BLGA at pH 2.65 were done using the assignment list of BLGA obtained from triple resonance spectra recorded at exactly the same conditions as those for template.[7] To transfer the assignments to pH 4.0, ^{1}H,^{15}N-HSQC NMR spectra of 400 μM BLGA WT were recorded at pH values of 2.65, 3.2, and 4.0, and the signals were followed during the titration to allow assignments at pH 4.0. These assignments are deposited in the Biological Magnetic Resonance Data Bank (BMRB, http://www.bmrb.wisc.edu/) entry 27668. For mapping of binding sites, a series of ^{1}H, ^{15}N-HSQC spectra were recorded for 100 μM BLGA WT or mutant protein and 15.5 mM AOSs at pH 2.65 or pH 4.0 prior to mixing in five steps with a BLGA sample not containing AOSs to give seven spectra in total recorded per protein sample at 0, 2.6, 5.2, 7.8, 10.4, 12.9, and 15.5 mM AOSs. Chemical shifts were in fast exchange and could be followed during the titration. Chemical shift perturbations were calculated to map the binding site on the surface of the protein by

$$\Delta\delta = \sqrt{(\Delta\delta H)^2 + (\Delta\delta N/5)^2}$$

where $\Delta\delta H = \Delta\delta H_{free} - \Delta\delta H_{obs}$ and $\Delta\delta N = \Delta\delta N_{free} - \Delta\delta N_{obs}$ are changes in the proton and nitrogen chemical shifts (in

DOI: 10.1021/acsomega.8b03532
ACS Omega 2019, 4, 6165−6174

ppm).[48] Significant chemical shift perturbation was defined as the average chemical shift perturbation plus one standard deviation.

Turbidimetry. The formation and assessment of solubility of BLGA/alginate particles were done as previously described.[18] Briefly, alginate, BLGA WT, or mutant proteins were dissolved in 50 mM NaPi pH 4.0. BLGA (1 mg mL^{-1} or 54 μM) was mixed with alginate (0−0.2 mg mL^{-1} or 0−5 μM using $\bar{M}_n$ = 40 kDa), incubated for 10 min at room temperature, and the turbidity was measured at 600 nm. Subsequently, the mixtures were centrifuged (20 000*g*, 20 min, 20 °C) and remaining soluble protein was determined spectrophotometrically at 280 nm.

■ ASSOCIATED CONTENT

Supporting Information

The Supporting Information is available free of charge on the ACS Publications website at DOI: 10.1021/acsomega.8b03532.

Primary structure of BLGA; TLC of alginate trisaccharides purification; details of alginate oligosaccharide structure determination (Figure S1); HSQC spectrum of the AOS sample (Figure S2); HSQC spectrum of AOS with the CLIP−HSQC spectrum (Figure S3); DQC−COSY spectrum (Figure S4), ROESY spectrum (Figure S5), HMBC spectrum (Figure S6), and HSQC−TOCSY spectrum of the AOS sample (Figure 7); NMR assignments of the alginate trisaccharides (Table S1); $^{1}H,^{15}N$-HSQC spectrum and chemical shift assignments of BLGA at pH 2.65 (Figure S8); correlation figure between our chemical shifts of β-lactoglobulin at pH 2.65 and an already published chemical shift list (Figure S9); fit of the classical one-site binding model to chemical shift perturbations (Figure S10); far-UV CD spectra of β-lactoglobulin WT and mutant proteins (Figure S11); $^{1}H,^{15}N$-HSQC spectrum and chemical shift assignments of BLGA at pH 4.0 (Figure S12); (Table S2) peak assignment for BLGA (Table S3); and difference between presented BLGA chemical shift assignment and the one by Uhrínová et al.'s (Table S4) unassigned residues of BLGA at pH 4.0 (PDF)

■ AUTHOR INFORMATION

Corresponding Authors

*E-mail: bbk@bio.ku.dk. phone: +45 3532 2081 (B.S.).
*E-mail: bis@bio.dtu.dk. phone: +45 4525 2740 (B.B.K.).

ORCID

Emil G. P. Stender: 0000-0003-2011-7452
Christian Kjeldsen: 0000-0002-0976-6622
Jens Ø. Duus: 0000-0003-3625-1250

Author Contributions

‖E.G.P.S. and J.B. contributed equally to this work.

Funding

The project StrucSat is supported by the Danish Council for Strategic Research (Grant no. 1308-00011B) and a third of a PhD stipend (to EGPS) from the Technical University of Denmark. The project HEXPIN is supported by the Independent Research Fund Denmark (Grant no. DFF—1335-00221). C.K. and J.Ø.D. acknowledge the Novo Nordisk foundation for funding (Grant no. 5371), and B.B.K., the Novo Nordisk Foundation SYNERGY grant. The AOS spectra were recorded at the NMR Center DTU and the protein spectra, at the structural biology and NMR Laboratory at BIO, UCPH, both supported by Villumfonden.

Notes

The authors declare no competing financial interest.

■ ACKNOWLEDGMENTS

Karina Jansen is thanked for technical assistance.

■ REFERENCES

(1) Flower, D. R. The lipocalin protein family: Structure and function. *Biochem. J.* **1996**, *318*, 1−14.
(2) Bordin, G.; Raposo, F. C.; de la Calle, B.; Rodriguez, A. R. Identification and quantification of major bovine milk proteins by liquid chromatography. *J. Chromatogr. A* **2001**, *928*, 63−76.
(3) Wu, S. Y.; Pérez, M. D.; Puyol, P.; Sawyer, L. β-Lactoglobulin binds palmitate within its central cavity. *J. Biol. Chem.* **1999**, *274*, 170−174.
(4) Yang, M. C.; Chen, N. C.; Chen, C. J.; Wu, C. Y.; Mao, S. J. T. Evidence for β-lactoglobulin involvement in vitamin D transport in vivo—role of the c-turn (Leu-Pro-Met) of β-lactoglobulin in vitamin D binding. *FEBS J.* **2009**, *276*, 2251−2265.
(5) Yang, M. C.; Guan, H. H.; Liu, M. Y.; Lin, Y. H.; Yang, J. M.; Chen, W. L.; Chen, C. J.; Mao, S. J. T. Crystal structure of a secondary vitamin D3 binding site of milk β-lactoglobulin. *Proteins: Struct., Funct., Genet.* **2008**, *71*, 1197−1210.
(6) Loch, J.; Polit, A.; Gorecki, A.; Bonarek, P.; Kurpiewska, K.; Dziedzicka-Wasylewska, M.; Lewinski, K. Two modes of fatty acid binding to bovine β-lactoglobulin-crystallographic and spectroscopic studies. *J. Mol. Recognit.* **2011**, *24*, 341−349.
(7) Uhrínová, S.; Uhrín, D.; Denton, H.; Smith, M.; Sawyer, L.; Barlow, P. N. Complete assignment of 1H, 13C and 15N chemical shifts for bovine β-lactoglobulin: secondary structure and topology of the native state is retained in a partially unfolded form. *J. Biomol. NMR* **1998**, *12*, 89−107.
(8) Brownlow, S.; Cabral, J. H. M.; Cooper, R.; Flower, D. R.; Yewdall, S. J.; Polikarpov, I.; North, A. C. T.; Sawyer, L. Bovine β-lactoglobulin at 1.8 ångstrom resolution - Still an enigmatic lipocalin. *Structure* **1997**, *5*, 481−495.
(9) Khan, S.; Ipsen, R.; Almdal, K.; Svensson, B.; Harris, P. Revealing the dimeric crystal and solution structure of β-lactoglobulin at pH 4 and its pH and salt dependent monomer-dimer equilibrium. *Biomacromolecules* **2018**, *19*, 2905−2912.
(10) Taulier, N.; Chalikian, T. V. Characterization of pH-induced transitions of β-lactoglobulin: Ultrasonic, densimetric, and spectroscopic studies. *J. Mol. Biol.* **2001**, *314*, 873−889.
(11) Brownlee, I. A.; Allen, A.; Pearson, J. P.; Dettmar, P. W.; Havler, M. E.; Atherton, M. R.; Onsøyen, E. Alginate as a source of dietary fiber. *Crit. Rev. Food Sci. Nutr.* **2005**, *45*, 497−510.
(12) Birch, J.; Harðarson, H. K.; Khan, S.; Van Calsteren, M.-R.; Ipsen, R.; Garrigues, C.; Almdal, K.; Abou Hachem, M.; Svensson, B. Effect of repeat unit structure and molecular mass of lactic acid bacteria hetero-exopolysaccharides on binding to milk proteins. *Carbohydr. Polym.* **2017**, *177*, 406−414.
(13) Du, X.; Dubin, P. L.; Hoagland, D. A.; Sun, L. Protein-selective coacervation with hyaluronic acid. *Biomacromolecules* **2014**, *15*, 726−734.
(14) Aberkane, L.; Jasniewski, J.; Gaiani, C.; Scher, J.; Sanchez, C. Thermodynamic characterization of acacia gum-β-lactoglobulin complex coacervation. *Langmuir* **2010**, *26*, 12523−12533.
(15) Girard, M.; Turgeon, S. L.; Gauthier, S. F. Quantification of the interactions between β-lactoglobulin and pectin through capillary electrophoresis analysis. *J. Agric. Food Chem.* **2003**, *51*, 6043−6049.
(16) Hosseini, S. M. H.; Emam-Djomeh, Z.; Razavi, S. H.; Moosavi-Movahedi, A. A.; Saboury, A. A.; Atri, M. S.; Van der Meeren, P. β-lactoglobulin-sodium alginate interaction as affected by polysaccharide depolymerization using high intensity ultrasound. *Food Hydrocolloids* **2013**, *32*, 235−244.

DOI: 10.1021/acsomega.8b03532
ACS Omega 2019, 4, 6165−6174

(17) Weinbreck, F.; de Vries, R.; Schrooyen, P.; de Kruif, C. G. Complex coacervation of whey proteins and gum arabic. *Biomacromolecules* **2003**, *4*, 293−303.
(18) Stender, E. G. P.; Khan, S.; Ipsen, R.; Madsen, F.; Hägglund, P.; Abou Hachem, M.; Almdal, K.; Westh, P.; Svensson, B. Effect of alginate size, mannuronic/guluronic acid content and pH on particle size, thermodynamics and composition of complexes with β-lactoglobulin. *Food Hydrocolloids* **2017**, *75*, 157−163.
(19) Fuenzalida, J. P.; Nareddy, P. K.; Moreno-Villoslada, I.; Moerschbacher, B. M.; Swamy, M. J.; Pan, S.; Ostermeier, M.; Goycoolea, F. M. On the role of alginate structure in complexing with lysozyme and application for enzyme delivery. *Food Hydrocolloids* **2016**, *53*, 239−248.
(20) Comert, F.; Malanowski, A. J.; Azarikia, F.; Dubin, P. L. Coacervation and precipitation in polysaccharide-protein systems. *Soft Matter* **2016**, *12*, 4154−4161.
(21) Xu, A. Y.; Melton, L. D.; Ryan, T. M.; Mata, J. P.; Rekas, A.; Williams, M. A. K.; McGillivray, D. J. Effects of polysaccharide charge pattern on the microstructures of β-lactoglobulin-pectin complex coacervates, studied by SAXS and SANS. *Food Hydrocolloids* **2018**, *77*, 952−963.
(22) Haug, A.; Larsen, B.; Smidsrod, O. A study of constitution of alginic acid by partial acid hydrolysis. *Acta Chem. Scand.* **1966**, *20*, 183−190.
(23) Haug, A.; Larsen, B.; Smidsrod, O. Studies on sequence of uronic acid residues in alginic acid. *Acta Chem. Scand.* **1967**, *21*, 691−704.
(24) Kristiansen, K. A.; Schirmer, B. C.; Aachmann, F. L.; Skjåk-Bræk, G.; Draget, K. I.; Christensen, B. E. Novel alginates prepared by independent control of chain stiffness and distribution of G-residues: Structure and gelling properties. *Carbohydr. Polym.* **2009**, *77*, 725−735.
(25) Aarstad, O. A.; Tøndervik, A.; Sletta, H.; Skjåk-Bræk, G. Alginate sequencing: An analysis of block distribution in alginates using specific alginate degrading enzymes. *Biomacromolecules* **2012**, *13*, 106−116.
(26) Koutina, G.; Ioannidi, E.; Melo Nogueira, B. M.; Ipsen, R. The effect of alginates on in vitro gastric digestion of particulated whey protein. *Int. J. Dairy Technol.* **2018**, *71*, 469−477.
(27) Hosseini, S. M. H.; Emam-Djomeh, Z.; Sabatino, P.; Van der Meeren, P. Nanocomplexes arising from protein-polysaccharide electrostatic interaction as a promising carrier for nutraceutical compounds. *Food Hydrocolloids* **2015**, *50*, 16−26.
(28) Garron, M. L.; Cygler, M. Structural and mechanistic classification of uronic acid-containing polysaccharide lyases. *Glycobiology* **2010**, *20*, 1547−1573.
(29) Zhang, Z.; Yu, G.; Guan, H.; Zhao, X.; Du, Y.; Jiang, X. Preparation and structure elucidation of alginate oligosaccharides degraded by alginate lyase from Vibro sp. 510. *Carbohydr. Res.* **2004**, *339*, 1475−1481.
(30) Kloareg, B.; Rochas, C.; Leonard, C.; Gey, C.; Heyraud, A.; Girond, S. NMR spectroscopy analysis of oligoguluronates and oligomannuronates prepared by acid or enzymatic hydrolysis of homopolymeric blocks of alginic acid. Application to the determination of the substrate specificity of *Haliotis tuberculata* alginate lyase. *Carbohydr. Res.* **1996**, *289*, 11−23.
(31) Kelly, S. M.; Jess, T. J.; Price, N. C. How to study proteins by circular dichroism. *Biochim. Biophys. Acta, Proteins Proteomics* **2005**, *1751*, 119−139.
(32) Sakurai, K.; Konuma, T.; Yagi, M.; Goto, Y. Structural dynamics and folding of β-lactoglobulin probed by heteronuclear NMR. *Biochim. Biophys. Acta, Gen. Subj.* **2009**, *1790*, 527−537.
(33) Cruz, A. G.; Cadena, R. S.; Alvaro, M. B. V. B.; Sant'Ana, A. S.; Oliveira, C. A. F.; Faria, J. A. F.; Bolini, H. M. A.; Ferreira, M. M. C. Assessing the use of different chemometric techniques to discriminate low-fat and full-fat yogurts. *LWT—Food Sci. Technol.* **2013**, *50*, 210−214.
(34) Dolinsky, T. J.; Nielsen, J. E.; McCammon, J. A.; Baker, N. A. PDB2PQR: An automated pipeline for the setup of Poisson-Boltzmann electrostatics calculations. *Nucleic Acids Res.* **2004**, *32*, W665−W667.
(35) Zhang, G.; Keiderling, T. A. Equilibrium and dynamic spectroscopic studies of the interaction of monomeric β-lactoglobulin with lipid vesicles at low pH. *Biochemistry* **2014**, *53*, 3079−3087.
(36) Harnsilawat, T.; Pongsawatmanit, R.; McClements, D. J. Characterization of β-lactoglobulin-sodium alginate interactions in aqueous solutions: A calorimetry, light scattering, electrophoretic mobility and solubility study. *Food Hydrocolloids* **2006**, *20*, 577−585.
(37) Tavel, L.; Andriot, I.; Moreau, C.; Guichard, E. Interactions between β-lactoglobulin and aroma compounds: different binding behaviors as a function of ligand structure. *J. Agric. Food Chem.* **2008**, *56*, 10208−10217.
(38) Gowda, V.; Foulke-Abel, J.; Agbo, H.; Bench, B. J.; Chae, J.; Russell, W. K.; Watanabe, C. M. H. Lipofuscin formation catalyzed by the milk protein β-lactoglobulin: Lysine residues in cycloretinal synthesis. *Biochemistry* **2017**, *56*, 5715−5719.
(39) Draget, K. I.; Braek, G. S.; Smidrod, O. Alginic acid gels - the effect of alginate chemical-composition and molecular-weight. *Carbohydr. Polym.* **1994**, *25*, 31−38.
(40) Lombard, V.; Bernard, T.; Rancurel, C.; Brumer, H.; Coutinho, P. M.; Henrissat, B. A hierarchical classification of polysaccharide lyases for glycogenomics. *Biochem. J.* **2010**, *432*, 437−444.
(41) Gao, Q.; Yang, J. Y.; Moremen, K. W.; Flanagan, J. G.; Prestegard, J. H. Structural characterization of a heparan sulfate pentamer interacting with LAR-Ig1−2. *Biochemistry* **2018**, *57*, 2189−2199.
(42) Srivastava, S.; Tirrell, M. V. *Advances in Chemical Physics*; Rice, S. A.; Dinner, A. R., Eds.; John Wiley and Sons, 2016; pp 499−544.
(43) Stender, E. G. P.; Koutina, G.; Almdal, K.; Hassenkam, T.; Mackie, A.; Ipsen, R.; Svensson, B. Isoenergic modification of whey protein structure by denaturation and crosslinking using transglutaminase. *Food Funct.* **2018**, *9*, 797−805.
(44) Dubois, M.; Gilles, K. A.; Hamilton, J. K.; Rebers, P. A.; Smith, F. Colorimetric method for determination of sugars and related substances. *Anal. Chem.* **1956**, *28*, 350−356.
(45) Gasteiger, E.; Hoogland, C.; Gattiker, A.; Duvaud, S.; Wilkins, M. R.; Appel, R. D.; Bairoch, A. Protein identification and analysis tools on the ExPASy server. In *The Proteomics Protocols Handbook*; Humana Press, 2005; pp 571−607.
(46) Kay, L. E.; Keifer, P.; Saarinen, T. Pure absorption gradient enhanced heteronuclear single quantum correlation spectroscopy with improved sensitivity. *J. Am. Chem. Soc.* **1992**, *114*, 10663−10665.
(47) Delaglio, F.; Grzesiek, S.; Vuister, G. W.; Zhu, G.; Pfeifer, J.; Bax, A. NMRpipe - a multidimensional spectral processing system based on UNIX pipes. *J. Biomol. NMR* **1995**, *6*, 277−293.
(48) Teilum, K.; Kunze, M. B. A.; Erlendsson, S.; Kragelund, B. B. (S)Pinning down protein interactions by NMR. *Protein Sci.* **2017**, *26*, 436−451.

DOI: 10.1021/acsomega.8b03532
ACS Omega 2019, 4, 6165−6174